Small-Signal Stability-Constrained Optimal Power Flow Using Eigenvalue Sensitivity Factors

Ahlem Aissa Berraies, Abbas Rabiee, and Innocent Kamwa
Department of Electrical and Computer Engineering, Laval University, Quebec, Canada
{ahlem.aissa-berraies.1, abbas.rabiee.1, innocent.kamwa.1}@ulaval.ca

***Abstract*—This paper presents an iterative small-signal stability constrained optimal power flow framework that explicitly incorporates small-signal stability into operational planning. The proposed formulation combines a conventional AC-Optimal Power Flow with a dynamic sensitivity model linking the dominant eigenvalues of the system state matrix to variations in generator active-power outputs and bus-voltage magnitudes. By linearizing the eigenvalue constraint around successive operating points, the method iteratively guides the optimization toward improved damping performance while preserving feasibility and cost efficiency. The approach is demonstrated on a standard 39-bus test system, showing consistent convergence and enhanced damping margins.**

***Index Terms*—Small-signal stability, optimal power flow, eigenvalues, stability, linearization**

I. Introduction

Maintaining secure and stable operation of power systems is a fundamental requirement, particularly as networks increasingly operate closer to their limits under varying generation and load conditions. Electromechanical oscillations may arise following small disturbances, and if not sufficiently damped, they can lead to loss of synchronism or instability [1]. To mitigate these phenomena, small-signal stability must be maintained, as it reflects the ability of the system to damp electromechanical oscillations effectively. Traditionally, small-signal stability has been enhanced through the use of damping controllers such as Power System Stabilizers (PSS), HVDC, and FACTS devices [2], [3]. In this context, the Optimal Power Flow (OPF) is used to determine the most economical and feasible operating point without explicitly considering the stability aspects. To overcome this limitation, several studies have proposed small-signal stability constrained optimal power flow (SSSC-OPF) models. [4] proposed an iterative redispatch algorithm in which the largest real part among system eigenvalues was evaluated numerically after each OPF solution. Although computationally simple, this two-stage approach treats the stability constraint externally, which limits its optimality and integration with system variables. In contrast, [5] introduced a stochastic OPF framework that incorporates voltage stability and small-signal stability into a unified OPF formulation. Other studies embedded stability indicators directly into the OPF by optimizing the spectral abscissa, i.e., the largest real eigenvalue. This was initially difficult due to its non-smooth behavior [6], but later work showed that the spectral abscissa is locally Lipschitz and differentiable almost everywhere, enabling its direct use in SSSC-OPF formulations [7]. In [8], the study focuses on rescheduling to enhance power transfer capability under small-signal stability constraints. The damping ratio of the least-damped mode was used as the small-signal stability index. On the other hand, [9] formulated the small-signal stability constraints by incorporating the real parts of all system eigenvalues. In [10], the SSSC-OPF formulation based on eigenvalue distribution was proposed, where the sensitivities of all eigenvalues were computed with respect to a reduced subset of dominant state variables, at the expense of increased computational complexity and the need for quasi-Newton updates. [11] introduced an alternative approach to the SSSC-OPF by replacing explicit eigenvalue constraints with a bilinear Matrix Inequality (BMI) representation of the stability condition, subsequently applying convex relaxations to obtain a semidefinite programming formulation (SDP). Additionally, [12] addressed the problem using heuristic optimization techniques, where the damping ratio of the critical mode is evaluated within PSO.

In this work, we develop a comprehensive SSSC-OPF formulation that explicitly couples the eigenvalues with the OPF decision variables. The aim is to ensure small-signal stability while minimizing total power losses. The proposed approach incorporates analytical sensitivities of the real and imaginary parts of the critical eigenvalues with respect to generator active power and voltage magnitudes, enabling targeted redispatch actions that improve eigenvalue locations without forcing excessively conservative operating conditions.

The remainder of this paper is organized as follows: Section II presents the overall problem formulation, including the mathematical definitions of small-signal stability used in the stability modelling. Section III introduces the proposed integrated SSSC-OPF approach, developed as a co-simulation between DIgSILENT PowerFactory and GAMS. Section IV presents a case study on the IEEE 39-bus system, discusses the obtained results with numerical validation, and Section V concludes the paper with future research directions.

II. Problem Formulation

A. General Formulation of the Power System and Optimization Problem

The power system can be represented by the following general form of differential-algebraic equations (DAEs):

This work was supported by the Natural Sciences and Engineering Research Council of Canada (NSERC) under Grant ALLRP 567550-21 through Université Laval, and by the Master's scholarship from Fondation Arbour.

979-8-3315-8138-1

$$
\begin{cases} \dot{x} = f(x, y, u) \\ 0 = g(x, y, u) \end{cases} \tag{1}
$$

where x denotes the vector of state variables (e.g., rotor angles, speeds), y represents the algebraic variables (e.g., bus voltages and angles), and u contains the control variables (e.g., generator voltage and power setpoints). The main objective of this work is to incorporate the small-signal stability of the grid into the OPF problem. Its general form is expressed as:

$$
\min_{x,y,u} \; C(P_{G_i}) \tag{2}
$$

Subject to:

$$
\begin{aligned} g(x, y, u) &= 0 \\ h(x, y, u) &\leq 0 \\ S(x, y, u) &= 0 \end{aligned} \tag{3}
$$

where $g(x, y, u)$ represents the nonlinear power flow equations of the network, $h(x, y, u)$ denotes the set of operational limits such as generation and voltage bounds, and $S(x, y, u)$ represents an implicit nonlinear function that links the eigenvalues of the system state matrix A to the OPF decision variables. These eigenvalues depend on the active power setpoints of the generator (P_{G_i}) and the terminal voltages (V_i). Unlike most SSSC-OPF formulations that constrain the real part of the critical eigenvalue, this work extends the linearization to both the real and imaginary components. This dual sensitivity formulation allows the optimization process to directly influence not only the damping of oscillatory modes but also their oscillation frequencies. Consequently, the proposed approach achieves improved control over the overall trajectory of eigenvalues in the complex plane while maintaining computational simplicity.

B. Small-Signal Stability Characterization

While the steady-state operating point is obtained by solving the algebraic equations $g(x, y, u) = 0$, the dynamic response of the system to small perturbations around this equilibrium is captured by the differential part $\dot{x} = f(x, y, u)$. To assess small-signal stability, these nonlinear equations are linearized around the steady-state operating point (x_0, y_0, u_0), resulting in a state-space representation that relates infinitesimal variations in the system states to their time derivatives.

$$
\begin{bmatrix} \Delta\dot{x} \\ 0 \end{bmatrix} = \begin{bmatrix} f_x & f_y \\ g_x & g_y \end{bmatrix} \begin{bmatrix} \Delta x \\ \Delta y \end{bmatrix}, \tag{4}
$$

where f_x, f_y, g_x, and g_y denote the corresponding Jacobian matrices of the nonlinear functions f and g evaluated at the operating point. This linearized model in (4) forms the basis for establishing the relationship between the system dynamics and the OPF control variables (P_{G_i}) and (V_i). By eliminating the algebraic variables Δy, the linearized state-space model of the system can be expressed as:

$$
\Delta\dot{x} = A_{\text{sys}} \Delta x, \quad A_{\text{sys}} = f_x - f_y g_y^{-1} g_x, \tag{5}
$$

where A_{sys} is the state matrix that describes the small-signal dynamics of the power system. Assuming a solution of the form $\Delta x = \phi e^{\lambda t}$, where ϕ is the mode shape and λ is the associated eigenvalue, substitution into (5) yields the eigenvalue problem $(A_{\text{sys}} - \lambda I)\phi = 0$. For a non-trivial solution ($\phi \neq 0$) to exist, the determinant of the coefficient matrix must be zero, leading to the characteristic equation:

$$
\det(\lambda I - A_{\text{sys}}) = 0. \tag{6}
$$

The resulting eigenvalues $\lambda_k = \sigma_k + j\beta_k$ represent the system modes, characterizing the local dynamic modes of the system:

- σ_k: real part of λ_k, representing the exponential damping;
- β_k: imaginary part of λ_k, corresponding to the oscillation frequency.

A mode k is stable if $\sigma_k < 0$, and its damping ratio ξ_k is given by:

$$
\xi_k = -\frac{\sigma_k}{\sqrt{\sigma_k^2 + \beta_k^2}}. \tag{7}
$$

III. Proposed Integrated SSSC-OPF Method

The optimization problem aims to minimize an objective function that is either economic (e.g., total generation cost) or technical (e.g., grid power losses) while ensuring compliance with both operational limits and small-signal stability constraints:

$$
\min_{P_{G_i}, V_i} \; C(P_{G_i}, V_i) \tag{8}
$$

subject to

$$
\begin{aligned} &g(x, y, u) = 0, \quad h(x, y, u) \leq 0 \\ &\sigma_k \leq \sigma_{\max}, \quad \xi_k \geq \xi_{\min}. \end{aligned} \tag{9}
$$

To relate eigenvalue variations to control variables, λ_k is expressed as a differentiable function of the OPF's decision variables:

$$
\Delta\lambda_k = \frac{\partial\lambda_k}{\partial P_{G_i}} \Delta P_{G_i} + \frac{\partial\lambda_k}{\partial V_i} \Delta V_i. \tag{10}
$$

By decomposing $\lambda_k = \sigma_k + j\beta_k$, both components are linearized as:

$$
\begin{bmatrix} \Delta\sigma_k \\ \Delta\beta_k \end{bmatrix} = \begin{bmatrix} S_{\sigma P} & S_{\sigma V} \\ S_{\beta P} & S_{\beta V} \end{bmatrix} \begin{bmatrix} \Delta P_{G_i} \\ \Delta V_i \end{bmatrix}, \tag{11}
$$

where the sensitivity matrices S_σ and S_β are obtained from first-order eigenvalue perturbations with respect to the OPF decision variables P_{G_i} and V_i around the base operating point. This linearization enables the tractable inclusion of stability indices within the OPF. Sensitivities with respect to voltage angles θ and reactive powers Q_{G_i} are omitted, as these variables are not independent OPF controls; their effects are implicitly reflected through variations in P_{G_i} and V_i.

A. SSSC-OPF Formulation

The base OPF aims to minimize total active power losses while satisfying the AC power flow equations and operational limits. It is formulated as follows:

$$
\min_{P_G, V_i} \; T_{\text{Loss}} = \sum_{i \in \mathcal{G}} P_{G_i} - \sum_{i \in \mathcal{B}} P_{D_i} \tag{12}
$$

979-8-3315-8138-1

subject to:

$$P_{G_i} - P_{D_i} = V_i \sum_{j\in\mathcal{B}} V_j (G_{ij}\cos\theta_{ij} + B_{ij}\sin\theta_{ij}) \tag{13}$$

$$Q_{G_i} - Q_{D_i} = V_i \sum_{j\in\mathcal{B}} V_j (G_{ij}\sin\theta_{ij} - B_{ij}\cos\theta_{ij}) \tag{14}$$

$$P_{G_i}^{\min} \le P_{G_i} \le P_{G_i}^{\max}, \quad Q_{G_i}^{\min} \le Q_{G_i} \le Q_{G_i}^{\max} \tag{15}$$

$$V_i^{\min} \le V_i \le V_i^{\max}, \quad |S_{ij}| \le S_{ij}^{\max} \tag{16}$$

$$P_{ij} = G_{ij}(V_i^2 - V_iV_j\cos\theta_{ij}) - B_{ij}V_iV_j\sin\theta_{ij} \tag{17}$$

$$Q_{ij} = -B_{ij}(V_i^2 - V_iV_j\cos\theta_{ij}) - G_{ij}V_iV_j\sin\theta_{ij} \tag{18}$$

$$P_{ij}^2 + Q_{ij}^2 \le S_{ij,\max}^2 \tag{19}$$

$$P_{ji}^2 + Q_{ji}^2 \le S_{ij,\max}^2 \tag{20}$$

The resulting OPF provides the steady-state operating point (x_0, y_0, u_0), including the optimal active power of the generator $P_{G_i}^{base}$ and the terminal voltages V_i^{base}, which serve as reference conditions for the subsequent small-signal stability analysis and linearization based on sensitivity. Once the base OPF is solved, integrated SSSC-OPF iterations are performed to enhance the small-signal stability margin while maintaining the new operating point as close as possible to the optimum point identified in the base OPF. To achieve this, the objective function is reformulated to minimize the deviation of generator active powers from the base OPF values:

$$\min_{P_G, V_G} C_{\text{iteration}} = \sum_{i\in\mathcal{G}} w_i \left(P_{G_i} - P_{G_i}^{base}\right)^2 \tag{21}$$

where w_i is a scalar weighting coefficient assigned to each generator to moderate its adjustment during the iterative update, preventing large deviations from $P_{G_i}^{base}$. The problem is solved subject to the same operational and network constraints defined in equations (13)–(20). In addition, the linearized eigenvalue-sensitivity relations are incorporated into the SSSC-OPF through the following constraints:

$$\sigma_k = \sigma_k^0 + \sum_{i\in\mathcal{G}} S_{\sigma_k, P_{g_i}} \left(P_{G_i} - P_{G_i}^0\right) + \sum_{i\in\mathcal{G}} S_{\sigma_k, V_i} \left(V_i - V_i^0\right) \tag{22}$$

$$\beta_k = \beta_k^0 + \sum_{i\in\mathcal{G}} S_{\beta_k, P_{g_i}} \left(P_{G_i} - P_{G_i}^0\right) + \sum_{i\in\mathcal{G}} S_{\beta_k, V_i} \left(V_i - V_i^0\right) \tag{23}$$

where:

- P_{G_i}, $P_{G_i}^0$: active power generation at generator i and its value at the previous iteration, respectively;
- V_i, V_i^0: voltage magnitude at generator bus i and its value at the previous iteration, respectively;
- $S_{\sigma_k, P_{g_i}}$, S_{σ_k, V_i}: sensitivity coefficients of the real part σ_k with respect to P_{G_i} and V_i, respectively;
- $S_{\beta_k, P_{g_i}}$, S_{β_k, V_i}: sensitivity coefficients of the imaginary part β_k with respect to P_{G_i} and V_i, respectively.

The first–order eigenvalue sensitivities used to obtain the coefficients in (22)–(23) are:

$$\frac{d\lambda_k}{dV_i} = \psi_k \left[-f_y \left(g_y^{-1} \frac{dg_y}{dV_i} g_y^{-1}\right) g_x\right] \phi_k \tag{24}$$

$$\frac{d\lambda_k}{dP_{G_i}} = \psi_k^\top \left[-f_y \left(g_y^{-1} \frac{dg_y}{dP_{G_i}} g_y^{-1}\right) g_x\right] \phi_k \tag{25}$$

where ϕ_k and ψ_k denote the right and left eigenvectors associated with eigenvalue λ_k, respectively. Thus, the coefficients S_σ and S_β in (22)–(23) are constant within each iteration, ensuring that the SSSC-OPF constraints remain linear in P_{G_i} and V_i.

B. Implementation of the integrated SSSC-OPF

The proposed integrated SSSC-OPF algorithm is executed via GAMS-DIgSILENT co-simulation, where GAMS performs the optimization, and DIgSILENT computes the matrix A_{sys} and its updated eigenvalues. The iterative workflow illustrated in Fig. 1 follows the steps below:

1) Solve the base AC-OPF to obtain the initial operating point (x_0, y_0), including P_G^0 and V_i^0.
2) Linearize the system around this point and compute the eigenvalues $\lambda_k^0 = \sigma_k^0 + j\beta_k^0$ of the state matrix A_{sys}.
3) Identify the critical eigenvalues based on σ_k and ξ_k.
4) Evaluate the first-order eigenvalue sensitivities with respect to P_{G_i} and V_i.
5) Integrate these sensitivities into the OPF model using the linearized relations (22) and (23).
6) Solve the integrated SSSC-OPF to update P_G and V_i.
7) Recompute A_{sys} and eigenvalues using the updated operating point, and repeat until:

$$\sigma_k \le \sigma_{\max}, \quad \xi_k \ge \xi_{\min}, \quad \forall k$$

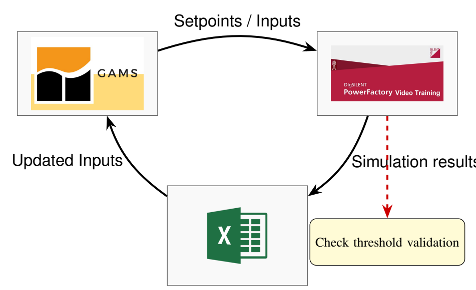

Fig. 1. Co-simulation workflow between GAMS, DIgSILENT with iterative convergence and physical validation.

Because the eigenvalue sensitivities rely on a first-order linearization around the current operating point, a single SSSC-OPF iteration is generally not sufficient to satisfy the stability constraints. The nonlinear eigenvalue trajectories computed by DIgSILENT often deviate from the linear predictions used by GAMS, and the identity of the critical mode may change during redispatch. Therefore, multiple iterations are required until the linearized OPF model and the nonlinear dynamic evaluation become consistent and all stability limits are simultaneously met. In this study, the damping ratio threshold was set to $\xi_{\min} = 3.75\%$, slightly higher than the 3.5% threshold used in [13], to examine the impact of enforcing a stricter stability requirement. The spectral abscissa limit, $\sigma_{\max}$, was chosen as -0.035 to ensure adequate modal damping without compromising operational feasibility. At each iteration, two

979-8-3315-8138-1

types of critical modes may be identified: (i) the modes with the largest real part and (ii) the modes with the lowest damping ratio, since these may correspond to different eigenvalues. The sensitivity coefficients used in (22)–(23) are obtained in DIgSILENT through finite perturbations of 1 to 5 MW for P_{G_i} and 0.01 pu for V_i. The resulting SSSC-OPF is solved as a nonlinear programming (NLP) problem in GAMS using the default NLP solver. The iterative process continues until both real-part and damping-ratio thresholds are satisfied.

IV. Results and Discussion

A. System under study

The proposed integrated SSSC-OPF approach is tested on the IEEE 39-bus benchmark system (Fig. 2). It consists of 39 buses, 10 generators, 19 loads, 34 transmission lines, and 12 transformers. The nominal frequency is 60 Hz, and the mains voltage level is 345 kV. The steady-state data used in this study correspond to the MATPOWER IEEE 39-bus test case [14].

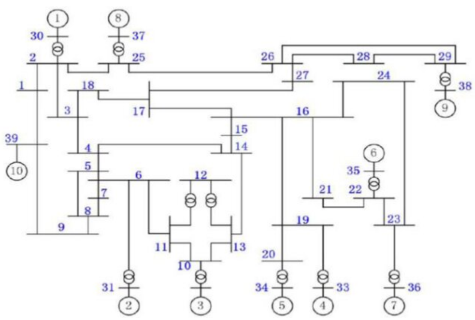

Fig. 2. IEEE 39-bus New England test system [10]

B. Obtained results

To assess the effectiveness of the proposed SSSC-OPF approach, Table I summarizes the evolution of the dominant eigenvalues, damping ratios, and total active power losses across the iterations. The generation cost is not included in the SSSC-OPF objective. Instead, it is evaluated afterward to quantify the economic impact of loss minimization under enhanced small-signal stability requirements. The reported improvements correspond to the current most critical modes at each iteration, as changes in the operating point modify the system Jacobian and may shift the identity of the least-damped eigenvalue. Overall, the real part of the critical eigenvalue improved from -0.0287 in the base case to -0.0362 after the final iteration, representing a 26% damping enhancement. In addition, the damping ratio of the oscillatory modes increased by 19%, meeting the secondary convergence criterion. These stability gains required coordinated adjustments in generator active powers and voltages, which increased the total loss from 29.7 MW to 40.9 MW, representing 0.67% of the total generated power. The resulting increase in generation cost was limited to 1.047%, confirming that enforced stability margins come with a modest economic impact. Fig. 3 and Fig. 4 complement the results of Table I by showing the trajectory of the dominant real eigenvalue and the oscillatory modes across the iterations. Fig. 3 illustrates the trajectory of the

TABLE I
Evolution of Dominant Eigenvalues and Damping Ratio During SSSC-OPF Iterations

Iteration	Mode	α (1/s)	β (rad/s)	ξ (%)	Total Loss (MW)	Total Cost ($)
Base	1 13/14	-0.02871 -0.24931	0 $\pm$7.875	100 3.16	29.70	127,937
1	1 13/14	-0.02872 -0.26020	0 $\pm$7.2088	100 3.61	29.851	127,865
2	1 13/14	-0.02874 -0.25788	0 $\pm$7.1587	100 3.60	29.917	128,055
3	1 13/14	-0.02887 -0.25356	0 $\pm$7.1558	100 3.54	33.228	128,439
4	1 11/12	-0.02858 -0.2716	0 $\pm$7.1898	100 3.77	32.717	128,172
5	1 12/13	-0.03196 -0.24843	0 $\pm$7.118	100 3.49	41.325	129,237
6	1 12/13	-0.03618 -0.27033	0 $\pm$7.173	100 3.77	40.909	129,277

dominant real eigenvalue over the six SSSC-OPF iterations, showing its progressive shift toward a more negative region as damping improves. Fig. 4 depicts the evolution of the oscillatory modes, highlighting how the imaginary and real parts jointly move further from the stability boundary as a result of the coordinated redispatch of generator active power and voltage.

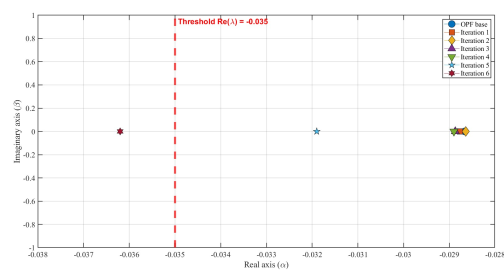

Fig. 3. Evolution of the Critical Eigenvalue across SSSC-OPF iterations

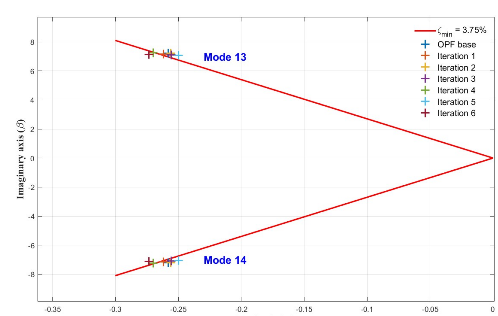

Fig. 4. Evolution of the Oscillatory Eigenvalues across SSSC-OPF iterations

Tables II and III show the evolution of generators' active power and terminal voltages across the SSSC-OPF iterations. The active power redispatch becomes progressively more pronounced, with G10 increasing from 1290.1 in the base OPF to 1775 MW in the final iteration. This variation indicates that achieving improved damping required a substantial shift from the initial OPF solution. During this process, the slack generator G2 first acted as the balancing unit that compensates for the mismatch, but gradually reduces its participation as G10 output rises, showing that the system shifted toward a more stable configuration. In parallel with the active power redispatch, the generator voltage magnitudes exhibit smaller variations throughout the iterations. Therefore, the observed damping improvement results from a coordinated adjustment of both active power and voltage, validating the importance of including voltage sensitivities in the SSSC-OPF formulation.

TABLE II
EVOLUTION OF GENERATOR ACTIVE POWERS DURING SSSC-OPF ITERATIONS (MW)

Gen	Iterations						
	Base	1	2	3	4	5	6
1	525.1	576.1	506.8	543.6	531.4	434.4	531.4
2	595.1	595.1	595.2	595.2	595.0	220	203.2
3	680.0	680.0	680.0	680.0	680.0	680	680.0
4	290.5	298.3	272.3	270.7	299.8	290.5	299.8
5	612.2	572.7	611.5	501.8	680.0	612.2	680.0
6	680.0	680.0	680.0	680.0	680.0	680	680.0
7	425.4	457.0	406.8	330.2	498.8	425.4	498.8
8	429.9	444.2	411.9	439.9	321.0	429.9	321.0
9	598.5	572.8	613.7	570.8	468.7	598.5	468.7
10	1290.1	1250.8	1348.9	1512.8	1375.2	1767.6	1775.2

TABLE III
EVOLUTION OF GENERATOR VOLTAGE MAGNITUDES DURING SSSC-OPF ITERATIONS (PU)

Gen	Iterations						
	Base	1	2	3	4	5	6
1	1.050	1.050	1.050	1.039	1.044	1.044	1.044
2	1.050	1.050	1.050	1.050	1.050	1.05	1.050
3	1.050	1.050	1.050	1.050	1.050	1.05	1.050
4	1.035	1.019	1.019	1.019	1.008	1.032	1.008
5	1.050	1.050	1.050	1.050	1.050	1.05	1.050
6	1.050	1.050	1.050	1.050	1.050	1.05	1.050
7	1.050	1.050	1.050	1.050	1.050	1.05	1.050
8	1.049	1.050	1.041	0.999	1.026	0.94	1.026
9	1.050	1.050	1.050	1.050	1.050	1.05	1.050
10	1.035	1.035	1.034	1.034	1.020	1.05	1.020

V. Conclusion and Future Work

In this work, an integrated SSSC-OPF formulation was developed that incorporates first-order eigenvalue sensitivities with respect to generator active power and voltage magnitudes, jointly considering the real and imaginary parts of the critical eigenvalues. This approach was implemented on the IEEE 39-bus system using DIgSILENT PowerFactory and GAMS, demonstrating a consistent enhancement of damping performance through coordinated adjustments of the generator active power outputs and terminal voltages. Despite the strong dynamic coupling between generators, the proposed method successfully improved the damping characteristics and shifted the critical eigenvalues into a more stable region. Importantly, the significant redispatch contribution of generator G2 is not a consequence of its slack-bus designation. Instead, it arises from its intrinsic dynamic influence on the critical modes and its operating limits. The sensitivity analysis confirms that G2 exhibits high participation in the least-damped modes, explaining its dominant role in the stability-oriented redispatch. The optimization process in this study was initialized from a stable operating point. In such cases, the goal of the SSSC-OPF is not to restore stability but rather to further enhance the existing damping margin. This makes the problem more challenging than stabilizing an initially unstable system. As a result, the resulting eigenvalue movements are more subtle and require careful coordination between active power redispatch and voltage adjustments. Future work will extend the framework to include transmission switching and renewable energy sources to further assess flexibility and stability enhancement in modern power systems.

References

[1] Berraies, A. A., Yari, S., Rabiee, A., & Kamwa, I. (2025, July). Comprehensive Assessment of the Impact of Large-Scale Solar Power Plants with WECC Controllers on Inter-Area Oscillations in the Power Grid. In 2025 IEEE International Conference on Environment and Electrical Engineering and 2025 IEEE Industrial and Commercial Power Systems Europe (EEEIC/I&CPS Europe) (pp. 1-6). IEEE.

[2] Wang, K. W., Chung, C. Y., Tse, C. T., & Tsang, K. M. (2002). Multimachine eigenvalue sensitivities of power system parameters. IEEE Transactions on Power Systems, 15(2), 741-747.

[3] Simo, J. B., Kamwa, I., Trudel, G., & Tahan, S. A. (2002). Validation of a new modal performance measure for flexible controllers design. IEEE transactions on power systems, 11(2), 819-826.

[4] Hamidreza Adeli, S., Rabiee, A., & Taghipour Boroujeni, S. (2020). Optimal re-dispatch of generating units ensuring small signal stability. IET Generation, Transmission & Distribution, 14(18), 3692-3701.

[5] Hamon, C., Perninge, M., & Söder, L. (2012). A stochastic optimal power flow problem with stability constraints—Part I: Approximating the stability boundary. IEEE Transactions on Power Systems, 28(2), 1839-1848.

[6] Li, P., Wei, H., Li, B., & Yang, Y. (2013). Eigenvalue-optimization-based optimal power flow with small-signal stability constraints. IET Generation, Transmission & Distribution, 7(5), 440-450.

[7] Li, P., Qi, J., Wang, J., Wei, H., Bai, X., & Qiu, F. (2016). An SQP method combined with gradient sampling for small-signal stability-constrained OPF. IEEE Transactions on Power Systems, 32(3), 2372-2381.

[8] Chung, C. Y., Wang, L., Howell, F., & Kundur, P. (2004). Generation rescheduling methods to improve power transfer capability constrained by small-signal stability. IEEE Transactions on Power Systems, 19(1), 524-530.

[9] Condren, J., & Gedra, T. W. (2006). Expected-security-cost optimal power flow with small-signal stability constraints. IEEE Transactions on Power Systems, 21(4), 1736-1743.

[10] Pai, A. (1989). Energy function analysis for power system stability. Springer Science & Business Media.

[11] Pareek, P., & Nguyen, H. D. (2021). A convexification approach for small-signal stability constrained optimal power flow. IEEE Transactions on Control of Network Systems, 8(4), 1930-1941.

[12] Pullaguram, D., Madani, R., Altun, T., & Davoudi, A. (2021). Small-signal stability-constrained optimal power flow for inverter dominant autonomous microgrids. IEEE Transactions on Industrial Electronics, 69(7), 7318-7328.

[13] Huang, Z., Wang, K., Wang, Y., Han, J., & Liang, J. (2024). Small-signal stability constrained optimal power flow considering eigenvalue distribution. Journal of Modern Power Systems and Clean Energy, 12(4), 1052-1062.

[14] Zimmerman, R. D., Murillo-Sánchez, C. E., & Thomas, R. J. (2010). MATPOWER: Steady-state operations, planning, and analysis tools for power systems research and education. IEEE Transactions on power systems, 26(1), 12-19.